

Theory and modeling of polarization switching in ferroelectrics

E. Klotins^{a,*}, J. Kaupužs^b

^a Institute of Solid State Physics, 8 Kengaraga Str., LV 1063 Riga, Latvia

^b Institute of Mathematics and Computer Science, University of Latvia, Raina Bulv. 29, LV 1459, Riga, Latvia

Available online 11 April 2005

Abstract

Kinetics of polarization response in ferroelectrics is reproduced within Langevin, Fokker–Planck and imaginary time Schrödinger equation techniques for energy functionals of growing complexity modeling an assembly of coarse grained particles with attractive first neighbor interaction. Symplectic integration based numerical approach captures dynamic hysteresis, polarization switching, and spatially extended stationary polarization. Solution of relevant nonstationary problem is adapted to large scale parallel computing.

© 2005 Elsevier Ltd. All rights reserved.

Keywords: Ferroelectric hysteresis

1. Introduction

Dynamics of metastable systems in general and the polarization response of ferroelectrics in particular is an active field of study based, for static solutions, on variation of Ginzburg–Landau type energy functionals. Extension of this standard approach toward kinetics of polarization includes additive Langevin noise term and transformation of the problem to Fokker–Planck equation for probability density of polarization.^{1–3} The Fokker–Planck equations may be derived in standard way for a wide variety of model energy functionals, nevertheless, its nonstationary solutions capturing external driving, spatial extension, and finite size effects is a challenge for the mathematical technique. In this context the Wentzel–Kramér–Brillouin (WKB) analysis based on mapping between Fokker–Planck and imaginary time Schrödinger equation and applicable for symplectic numerical integration has received a renewed attention.⁴ Some recent results for metastable systems specified by quartic energy functional and modeling, in some extent, dynamic hysteresis in a system with periodic boundary conditions are given in.⁵ Taking in game the ferroelectric phase instability requests a more complex than the Ginzburg–Landau energy

functional⁶ modeling a set of interacting Landau-type coarse grained blocks. Specific feature of relevant Fokker–Planck equation is strong nonlinearity which, nevertheless, can be managed in nonperturbative fashion in the course of symplectic integration⁷. In this work we give a short insight in this kind of analysis with special emphasis on polarization response and exhibiting a nontrivial and contrainuitive behavior as originated by cooperative effect of thermal noise and external driving. Our main results concern dynamic hysteresis (Section 2), polarization switching (Section 3), and spatial extension (Section 4). Physical content and capabilities of the proposed mathematical technique for more complex problems is shortly discussed in Section 5.

2. Definitions and concepts: dynamic hysteresis

Definitions start with the standard Ginzburg–Landau energy functional for double well (dimensionless) potential $U(P,t) = -1/2P^2 + 1/4P^4 + 1/2(\nabla P)^2 - \lambda(t)P$ routinely applied to uniaxial ferroelectrics, the Langevin kinetic equation with δ -correlated Gaussian noise term, and Fokker–Planck equation for probability density of polarization $\rho(P,t)$

$$\frac{\partial \rho(P,t)}{\partial t} = \Gamma \frac{\partial}{\partial P} \left(\frac{\delta U}{\delta P} \rho(P,t) \right) + k_B T \Gamma \frac{\partial^2 \rho(P,t)}{\partial P^2}. \quad (1)$$

* Corresponding author. Tel.: +371 718 78 66; fax: +371 713 27 78.

E-mail addresses: klotins@cfi.lu.lv (E. Klotins), kaupuzs@latnet.lv (J. Kaupužs).

Here Γ , T are the kinetic coefficient and temperature, correspondingly, Θ the diffusion coefficient (noise strength) bounding together parameters of the system and $\lambda(t)$ specify the time dependent driving voltage. In further calculations, Eq. (1) is transformed in dimensionless form and the multivariate nature of the probability density $\rho(\{P\}, t)$ is not exposed explicitly as motivated by later split of the multivariate probability density in statistically independent parts

$$\dot{\rho}(P, t) = \frac{\partial}{\partial P} \left(\frac{\delta U}{\delta P} \rho(P, t) \right) + \Theta \frac{\partial^2 \rho(P, t)}{\partial P^2} \quad (2)$$

The concept is to transform Eq. (2) in imaginary time Schrödinger equation and its subsequent symplectic integration. Omitting temporarily the gradient term $(\nabla P)^2/2$ and addressing to the quartic model we use the standard WKB ansatz $\rho(P, t) = \exp[-U(P)/2\Theta]G(P, t)$ mapping Fokker–Planck and imaginary time Schrödinger equations. What we search is the auxiliary function

$$\frac{\partial G(P, t)}{\partial t} = \left[\Theta \frac{\partial^2}{\partial P^2} + V(P) \right] G(P, t) \quad (3)$$

Here the potential operator $V(P)$ reads as:

$$V(P) = \left[-\frac{1}{4\Theta} [U'(P)]^2 + \frac{1}{2} U''(P) \right] \quad (4)$$

and the auxiliary function $G(P, t)$ Eq. (3) unfolds polarization kinetics through the first moment of probability density $\rho(P, t)$ Eq. (2). Analytical part of computations is completed by recurrence relation valid for a small time slice Δt

$$G(P, t + \Delta t) = \exp \left[\Delta t \left(\Theta \frac{\partial^2}{\partial P^2} + V(P) \right) \right] G(P, t) \quad (5)$$

Example solutions for quartic toy models are given in.^{4,7} Computing details include correctable integration algorithms⁸ and replacing the exponential operator $\exp[\Theta \Delta t (\partial^2)/(\partial P^2)]$ in Eq. (5) by its Cayley's form⁷ resulting in matrix recurrence equation for the auxiliary function, namely

$$\begin{aligned} & \left(1 - \frac{\Theta \Delta t}{2} \frac{\partial^2}{\partial P^2} \right) G(P, t + \Delta t) \\ &= \exp \left[\frac{\Delta t}{2} V + \frac{\Delta t^3}{48} (\nabla V)^2 \right] \left(1 + \frac{\Theta \Delta t}{2} \frac{\partial^2}{\partial P^2} \right) \\ & \quad \times \exp \left[\frac{\Delta t}{2} V + \frac{\Delta t^3}{48} (\nabla V)^2 \right] G(P, t) \end{aligned} \quad (6)$$

Example solution for the hysteresis at harmonic driving $\lambda(t) \propto \sin(\Omega t)$ modeled by Eq. (6) shown in Fig. 1 (dots) exhibits zero ground state as its stationary point. In contrast, the eigenfunction solution of Eq. (2) is combined with Floquet function technique² and counts in exclusively the zero and first order eigenfunctions. Nevertheless, the compatibility is fairly good and reassures correctness of the approach

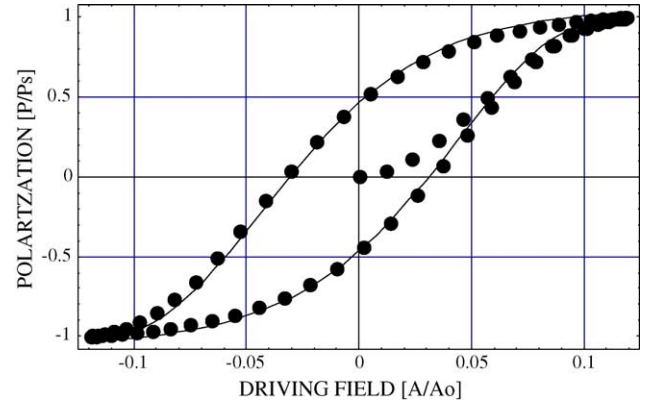


Fig. 1. Dynamic hysteresis under harmonic driving: comparison of semiadiabatic approach² (line) and symplectic integration (dots). Parameters of the problem: amplitude of the driving voltage $h = 0.309h_0$, frequency $\Omega = 10^{-3}$, $\Theta = 1/20$, $\lambda(t) = \sin(\Omega t)$, and $h_0 = 2/\sqrt{27}$ is the static coercive field.

Eqs. (1)–(6). The underlying physics concerns noninteracting coarse grained blocks with Ginzburg–Landau type internal kinetics. Bifurcation of the stationary ground state is demonstrated in Section 3.

Spatial extension formally is introduced by returning the gradient term in energy density $U(P, t)$ ⁹ and yields analytical estimates connecting alterations of polarization with symmetry violation of the $V(P)$ -potential Eq. (4). The effect of driving field is enhanced by a term proportional to the second spatial derivative of polarization contributing in symmetry violation and favoring polarization switching in vicinity of domain boundaries. This approach gives an insight in a long-standing problem of ferroelectric domain switching that appears far below the classic coercive voltage. In more detail, this approach requires split of the multivariate probability density in statistically independent parts as based on series representation of its first moment and shown in Section 4.

3. Nonlocality: polarization switching

Bifurcation of the ground state and the remnant polarization is recovered by energy functional modeling an assembly of overdamped anharmonic oscillators.⁶ On physical grounds it concerns a system of coarse grained particles (blocks) with attractive interaction modeled by the Hamiltonian

$$H = U(P_i) + \frac{\varepsilon}{2N} \sum_k^N (P_k - P_i)^2 \quad (7)$$

The corresponding Fokker–Planck equation reads as

$$\dot{\rho}(P, t) = \frac{\partial}{\partial P} \left[U'(P, t) + \Theta \frac{\partial}{\partial P} \right] \rho(P, t) \quad (8)$$

here each i th block is described by equal kinetics and $\varepsilon > 0$ denotes the strength of attractive mean-field type coupling. For quartic potential $U(P, t) = -P^2/2 + P^4/4 + \varepsilon/2 [P - \bar{P}(t)]^2 - P\lambda(t)$ and at appropriate interaction the

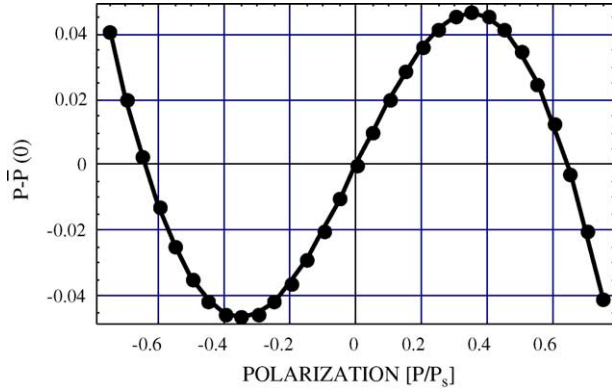


Fig. 2. Schematic plot of $P - \bar{P}(0)$ as a function of polarization P (in P_s units). The stationary polarization $\bar{P}(0)$ is recovered by intersection of $P - \bar{P}(0)$ plot with the p -axis exhibiting two stable solutions at $\bar{P} = \pm 0.64$ and an unstable solution at $\bar{P} = 0$. Parameters of the model: $\varepsilon = 0.07$, $\lambda = 0$, $\Theta = 1/20$.

system exhibits two remnant (stationary) states as

$$\rho(P, 0) = \frac{\exp[-U_1(P, 0) + U_2(P, 0)/\Theta]}{\int \exp[-U_1(P, 0) + U_2(P, 0)/\Theta] dP} \quad (9)$$

Here $U_1(P, t) = -(P^2/2) + (P^4/4) - P\lambda(t)$, $U_2(P, 0) = \varepsilon/2[P - \bar{P}(0)]^2$ and the denominator provides normalization of the probability distribution $\int \rho(P, 0) dP = 1$. The stationary (initial) value of the first moment of polarization density $\bar{P}(0)$ is found by integrating Eq. (9) over P with $\bar{P}(0)$ as a parameter. In $P, P - \bar{P}(0)$ frame the exact value of $\bar{P}(0)$ exhibit itself as the intersection of $P - \bar{P}(0)$ plot with the P -axis as shown in Fig. 2.

Specific for the mathematical technique is nonlinearity of Eq. (8) the potential $U(P, t)$ term of which comprises the first moment of probability density. Nevertheless, nonperturbative temporal solution of this nonlinear problem is found by introducing recursion-specific approximation of the first moment $\bar{P}(t_i + \Delta t) = \bar{P}(t_i) + q_i \Delta t$ and selfconsistent calculation of its time derivative q_i . Long time zero field limit of this solution is found in⁶ stating that (at appropriate interaction constant) the system always reaches one of the stationary states regardless of the initial condition. Extension of this result for periodic driving is studied in¹⁰ and equilibrium properties are found similar to those of shifted undriven system. The probability that a metastable system resides within a domain of attraction is estimated in¹¹. Essential solution for polarization reverse is illustrated in Fig. 3 for a system with initially positive remnant polarization. The reverse is initiated by a negative saw tooth shaped pulse specified by -0.1 , -0.05 , and -0.027 dimensionless amplitudes scaled after $2/\sqrt{27}$ static coercive field.² Both short (100π) and moderate length ($1000\pi/2$) pulses apply for each driving amplitude. Time propagation of polarization response starts from $\bar{P}_{r+} = 0.64$ remnant polarization and finishes at a value $\bar{P} < \bar{P}_{r+}$ as the driving turns to zero with subsequent relaxation toward one of the stationary states. The sign of remnant polarization approached by the system depends on the sign

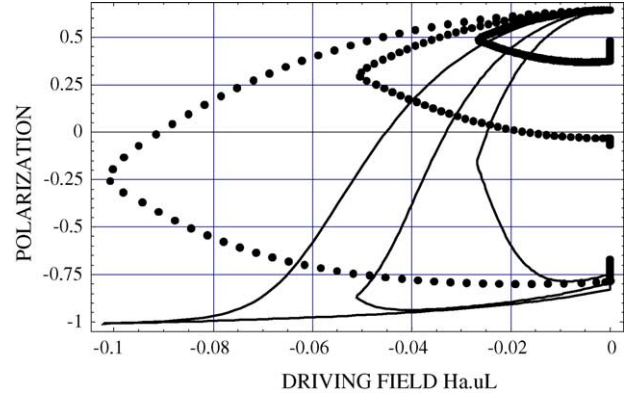


Fig. 3. Polarization switching from $\bar{P}_{r+} = +0.64$ stationary initial state to the $\bar{P}_{r-} = -0.64$ final state initiated by -0.1 , -0.05 , and -0.027 saw tooth shaped pulse of short (dots) and moderate (dashed lines) length.

of the first moment of probability distribution at the time instant the driving is switched off, namely $\bar{P}_{\lambda=0} > 0$ yields $\bar{P}_{t \rightarrow \infty} \rightarrow \bar{P}(0)$, and otherwise. The first case is confirmed by the -0.027 short pulse (dots). Otherwise, the polarization plot corresponding to -0.027 moderate length pulse (dashed line) approaches to $\bar{P}_{r-} = -0.64$ from below in accord with the H-theorem of global stability. Similarly, the polarization plot corresponding to -0.05 short pulse (dots) exhibit $\bar{P}_{\lambda=0} < 0$ and approaches to $\bar{P}_{r-} = -0.64$ from above also in accord with the H-theorem. All driving amplitudes exceeding -0.05 are overcritical as manifested by the rest of plots in Fig. 3.

4. Spatial extension: first neighbor interaction

Spatial extension, lost in mean field approach Eq. (7), is restored ad hoc by assuming that (i) the system consists of large but finite number of coarse grained blocks with internal kinetics obeying Eq. (7) at $\varepsilon = 0$, and (ii) the interaction between blocks is restricted within first neighbor so addressing the problem to ensemble of interacting blocks. The relevant model Hamiltonian

$$H \equiv \sum_i^N \left\{ U_i + \frac{\varepsilon}{2} ((\bar{P}_{i+1}(t) - P_i)^2 + (\bar{P}_{i-1}(t) - P_i)^2) \right\} \quad (10)$$

Here $U_i = -1/2 P_i^2 + 1/4 P_i^4 - \lambda(t) P_i$, the first moments of probability density \bar{P}_k are evaluated selfconsistently in the recursion-specific approximation technique applied to spatial mesh. Relevant Fokker–Planck equation reads as

$$\begin{aligned} \dot{\rho}(P_i, t) = & -\frac{\partial}{\partial P_i} \\ & \times \left[-\frac{\partial \Phi_i}{\partial P_i} \rho(P_i, t) + \varepsilon (\bar{P}_{i+1}(t) - 2P_i + \bar{P}_{i-1}(t)) \rho(P_i, t) \right] \\ & + \Theta_i \frac{\partial^2}{\partial P_i^2} \rho(P_i, t) \end{aligned} \quad (11)$$

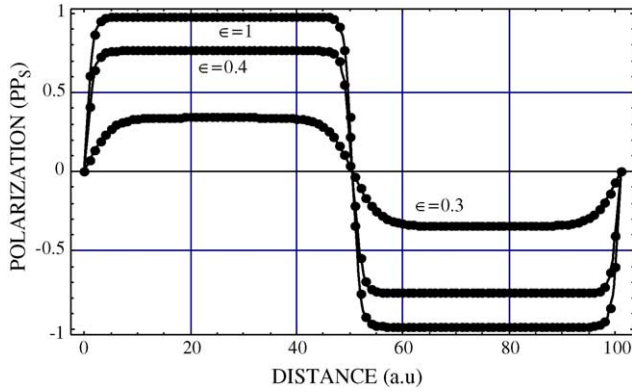


Fig. 4. Example solution for 180° domains within a 1-D region with zero boundary conditions and various interaction constants.

and its stationary solution is shown in Fig. 4 for zero boundary conditions and various interaction between blocks as a parameter. Starting values $\bar{P} = \pm 1$ are obtained from the static approach^{12,13}.

Nonstationary solution of Eq. (11) starts with the WKB ansatz $\rho(P_i, t) = \exp[-F(P_i, t)]G(P_i, t)$ and the relation for the exponential factor is given by $F = [\varepsilon P_i(\bar{P}_{i-1} - P_i + \bar{P}_{i+1}) - U(P_i)]/(2\Theta)$ generating a set of imaginary time Schrödinger equations for the auxiliary functions

$$\hat{G}(P_i, t) = (T_i + V_{1i} + V_{2i} + K_i)G(P_i, t) \quad (12)$$

defined over the spatial mesh $i \in [1, i_{\max}]$. Here the kinetic $T_i = \Theta(\partial^2/\partial P_i^2)$ and first potential $V_{1i} = -1/4\Theta_i(\partial U_i/\partial P_i)^2 + 1/2(\partial^2 U_i/\partial P_i^2)$ terms in Eq. (12) are regular ones, Eq. (4). The supplementary potential terms, accounting for interaction yields

$$V_{2i} = \frac{\varepsilon}{4\Theta} \left(4\Theta_i - (2P_i - \bar{P}_{i-1}(t) - \bar{P}_{i+1}(t)) \left(2P_i - \varepsilon(\bar{P}_{i-1}(t) + \bar{P}_{i+1}(t)) + 2\frac{\partial U}{\partial P_i} \right) \right) \quad (13)$$

$$K_i = \frac{[-\varepsilon P_i \dot{\bar{P}}_{i-1}(t) - \varepsilon P_i \dot{\bar{P}}_{i+1}(t) + \dot{\Phi}_i]}{2\Theta} \quad (14)$$

improving the previous analytical estimates for polarization switching⁹ in more detail. Firstly, the impact of $P_i(2P_i - \bar{P}_{i-1}(t) - \bar{P}_{i+1}(t))$ -type terms in Eq. (13) exhibit maximum in the first order of interaction factor ε . Secondly, the interaction contributes even if the second spatial derivative of polarization is zero. Thirdly, the impact of alternate driving Eq. (14) is supplemented by terms proportional to the interaction factor ε . Representation of Eq. (12) in terms of symplectic integration Eq. (6) includes series expansion of the first moments of probability density $\bar{P}_i(t)$ similarly to this in Section 3 resulting in a set of coupled algebraic equations for the expansion coefficients. Numerical solution of Eqs. (12)–(14) is a subject of large scale modeling and is out of scope of this work.

5. Summary and discussion

Thermal noise activated nonadiabatic behavior of metastable systems is investigated in the context of electric hysteresis and polarization switching in ferroelectrics. Main focus is made on the mathematical technique as based on the Langevin–Fokker–Planck–imaginary time Schrödinger scheme addressing the problem to matrix recurrence relations in the course of symplectic integration. The definition of physical system is given by energy functionals of growing complexity and the test solutions captures arbitrary alternate driving, polarization switching, and spatial inhomogeneity. Key features of this mathematical technique are demonstrated by dynamic hysteresis modeled by quartic energy functional. A more realistic energy functional for an assembly of coarse grained particles with attractive interaction captures bifurcation of stationary states and divergence of relaxation time. Nonperturbative solution of this strictly nonlinear problem is exemplified by polarization switching and is handled by series expansion of the first moments of probability density so readdressing evaluation of its coefficients to standard algebra. This trick allows spatial extension and makes the density distribution in different spatial points statistically independent. Based on this property the stationary solution for finite size problem is demonstrated by the third model energy functional with interaction terms restricted to first neighbors so maintaining the spatial inhomogeneity of polarization field. The relevant nonstationary problem is addressed to symplectic integration adapted to large scale parallel computing. Whereas, the physical content is reduced to display exclusively the properties of interest there are no principal restrictions for supplementary terms in the energy functional as well as for dimensionality of the problem, and boundary and initial conditions. Examples

of supplementary terms include acoustic interactions¹⁴ and the impact of charged defects accounted for by the Poisson equation. The ordinary boundary conditions are available automatically due the real space mesh. Concluding, it is shown how the Langevin, Fokker–Planck and imaginary time Schrödinger equation techniques can be preceded elegantly in terms of symplectic integration even for nonlocal and nonlinear problems and has a potential to nonadiabatic response in ferroelectrics.

Acknowledgement

This work was partially supported by the Contract No. ICA1-CT-2000-70007 of European Excellence Center of Advanced Material Research and Technology (Riga).

References

1. Liu, J.-M., Li, Q. C., Wang, W. M., Chen, X. Y., Cao, G. H., Liu, X. H. *et al.*, Scaling of dynamic hysteresis in ferroelectric spin systems. *J. Phys. Condens. Matter*, 2001, **13**(6), L153–L161.
2. Talkner, P., Stochastic resonance in the semiadiabatic limit. *N. J. Phys.*, 1999, **1**, 4.1–4.25.
3. Klotins, E., Polarization Reversal in Ferroelectrics: Stochastic Analysis. *Ferroelectrics*, 2003, **296**, 209–220.
4. Caroli, B., Caroli, C. and Roulet, B., Diffusion in a Bistable Potential: A Systematic WKB Treatment. *J. Stat. Phys.*, 1979, **21**(4), 415–437.
5. Kaupužs, J. and Rimshans, J., Polarization kinetics in ferroelectrics with regard to fluctuations. arXiv: Cond-Mat/0405124 v1; May 2004.
6. Shiino, M., Dynamical behavior of stochastic systems of infinitely many coupled nonlinear oscillators exhibiting phase transitions of mean-field type: *H* theorem on asymptotic approach to equilibrium and critical slowing down of order-parameter fluctuations. *Phys. Rev. A*, 1986, **36**(5), 2393–2412.
7. Watanabe, N. and Tsukada, M., Fast and stable method for simulating quantum electron dynamics. *Phys. Rev. E.*, 2000, **62**, 2914.
8. Siu A. Chin, Quantum Statistical Calculations and Symplectic Corrector Algorithms. arXiv: Cond-Mat/0312021 v11; December 2003.
9. Klotins, E., Relaxation dynamics of metastable systems: application to polar medium. *Physica A*, 2004, **340**, 196–200.
10. Drozdov, N. and Morillo, M., Validity of basic concepts in nonlinear cooperative Fokker-Planck models. *Phys. Rev. E*, 1995, **54**(4), 3304–3313.
11. Talkner, P., Luczka, J., Rate description of Fokker-Planck processes with time dependent parameters. arXiv: Cond-Mat/0307498 v121; Jul 2003.
12. Wan, Y. S., Wei-Heng, S. and Aksay Ilhan, A., Size dependence of the ferroelectric transition of small BaTiO₃ particles: Effect of depolarisation. *Phys. Rev. B*, 1994, **50**(21), 15575–15585.
13. Bratkovsky, A. M. and Levanyuk, A. P., Easy Collective Polarization Switching in Ferroelectrics. *Phys. Rev. Lett.*, 2000, **85**(21), 4614–4617.
14. Hlinka, J. and Klotins, E., Application of elastostatic Green function tensor technique to electrostriction in cubic, hexagonal and orthorhombic crystals. *Phys. Condens. Matter*, 2003, **15**, 5755–5764.